

Equilibrium and levitation of dust in a collisional plasma with ionization

S. V. Vladimirov* and N. F. Cramer

Department of Theoretical Physics, School of Physics, The University of Sydney, New South Wales 2006, Australia

(Received 23 February 2000; revised manuscript received 11 April 2000)

The equilibrium, stability, and trapping of dust particles associated with vertical motions in the plasma sheath and presheath are calculated, taking into account the dependence of the variables (such as dust charge, ion flow velocity, etc.) on the local position in the sheath or presheath region of a collisional plasma with an ionization source. It is demonstrated that an increase of the rate of ionization considerably influences the equilibrium positions of dust grains, shifting them toward the electrode as well as increasing the maximum possible (equilibrium) levitation grain size.

PACS number(s): 52.25.Zb, 52.25.Vy, 52.35.Fp, 52.40.Hf

I. INTRODUCTION

The structures formed by charged dust grains in a low-temperature weakly ionized plasma have attracted considerable recent interest, associated primarily with the first experiments on “dust-plasma crystals” [1–5] as well as later with other self-organized formations such as dust clouds, “drops,” “voids,” etc. [6–13]. Under typical laboratory conditions, dust particles are negatively charged and usually levitate in the sheath or presheath region under the balance of gravitational, electrostatic (due to the sheath electric field), and plasma (such as the ion drag) forces. The ion flow, in addition to a direct (dragging) influence which can be one of the major forces supporting the formation of dust voids [9,10], is also responsible for the generation of associated collective plasma processes that can strongly affect the vertical arrangement of the grains, not only in the case of supersonic flows when a wake field is generated [14–17], but also in the case of subsonic velocities of plasma ions [18,19]. On the other hand, molecular dynamic simulations [20] have clearly demonstrated a sequence of phase transitions associated with vertical arrangements of dust grains when the strength of the confining (in the vertical dimension) parabolic potential is changed. The vertical positioning of the dust grains is directly connected with the possible equilibrium of the system.

It is well known that the charge of dust particles, which is one of the most important characteristics for the trapping and interaction of dust grains, appears as a result of various processes in the surrounding plasma, mainly (under typical laboratory conditions) due to electron and ion current onto the grain surfaces (see, e.g., Ref. [21]). Thus the first step in any research on properties of dust in a plasma is the adequate description of the surrounding plasma. Here, we note that, in general, there are two situations of interest: (i) the dust particles do not affect significantly the properties of the plasma they are embedded in (this usually corresponds to low number densities of the dust component, i.e., to a lower number of dust particles), and (ii) the dust component is relatively dense, thus changing significantly the field and density dis-

tributions of the surrounding plasma. Note that the second case corresponds to such interesting self-organized dust-plasma structures as voids and clouds in the dust-plasma sheaths [9–12].

In this paper, we are mainly concerned with a plasma with a rarefied dust component, i.e., we are assuming that dust charges and electric fields do not change the plasma parameters significantly. We therefore consider the case of essentially isolated dust grains (the intergrain distance exceeds the plasma Debye length), with a low total number of dust particles. Thus the first step in our study is the modeling of those plasma regions where we expect the dust particles to be trapped, the sheath and presheath regions of the discharge.

Due to relatively high neutral gas pressures (often more than 50 mTorr for typical dust-plasma experiments), the laboratory plasma is strongly influenced by the effects of ion-neutral collisions. Thus the simplest mathematical approach relevant for collisionless plasmas [22–24] is not fully appropriate in this case. On the other hand, the correct description of collisional effects involves the speed of the ion flow and therefore naturally depends on the properties of the region (sheath or presheath) we are interested in. While in the sheath region, where the speed of the ion flow is expected to exceed the ion sound velocity, a simple approximation [25] describing ion-neutral collisions can be used, in the total presheath/sheath region more sophisticated approaches are necessary [26,27]. In this paper, we use an advanced model of momentum transfer between the ion and neutral species, which describes ion-neutral collisions on the basis of kinetic theory, without semiempirical approximations [28].

Another important issue is the rate of ionization. It was demonstrated experimentally (see, e.g., [9,11]) that an increase of the ionization rate leads to an increased size of the dust-free void region, moving the equilibrium position of the dust cloud closer to the electrodes. Thus we expect that, even in the case of dust in a plasma with a negligible influence of the dust on the plasma and sheath parameters, the equilibrium positions of the grains are affected by the ionization rate. Therefore we also include plasma ionization in our equations.

Previously, various models of dust levitation in the low-temperature plasma discharge sheath region were numerically considered (see, e.g., [12,29–33]). Note that the previ-

*Email address: S.Vladimirov@physics.usyd.edu.au; URL: <http://www.physics.usyd.edu.au/~vladimi>

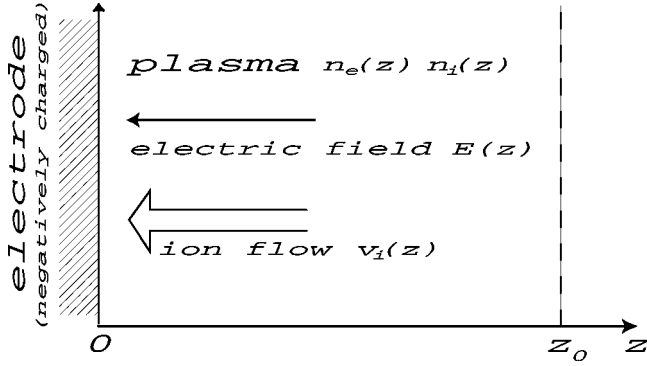


FIG. 1. Sketch of the one-dimensional simulation configuration.

ous models deal with the collisionless [32,33] or collisional [12] fluid cases without ionization, the kinetic (i.e., coupled Poisson-Vlasov equations) case [31] without collisions in the vicinity of a dust grain, particle-in-cell simulations [30] of a uniform, steady state dc plasma where plasma particle losses are assumed to be exactly balanced by a constant ionization source, or a hybrid model [29] combining Monte Carlo with fluid simulation, with the latter ignoring the equations of motion of the plasma particles. In this paper, we present a self-consistent fluid model of (rarefied) dust levitation and equilibrium in a collisional plasma sheath taking into account plasma ionization.

Possible vertical motions of the dust can lead to the disruption of the equilibrium position of the grains. Note that most of the previous analytical models considering vertical lattice vibrations [34,35], as well as numerical models studying phase transitions [20] in the dust-plasma system, dealt with dust grains of a constant charge. Recently [33], we demonstrated that the dependence of the dust particle charge on the sheath parameters has an important effect on the oscillations and equilibrium of dust grains in the vertical plane, leading to a disruption of the equilibrium position of the particle and a corresponding transition to a different vertical arrangement. However, we used the simplest model of a collisionless plasma sheath, with supersonic velocities of the ion flow. In this paper, we study the whole range of possible velocities of the ion flow, treating the sheath problem self-consistently and investigating possible dust trapping as well as the disruption of the equilibrium that may occur at various positions corresponding to not only supersonic, but also subsonic, ion flow velocities at the position of the dust grain in a collisional plasma with an ionization source.

II. PLASMA MODEL

The plasma consists of electrons and singly charged ions, with a uniform background neutral gas. The dust grains are assumed to have no effect on the sheath and presheath structure. We consider the one-dimensional configuration sketched in Fig. 1: the electrode, which is supposed to be at the constant potential -7 V, is located at the origin of the reference frame; the end of the simulation volume is at z_0 outside the sheath. All variables of interest are functions of the distance z , namely, the sheath potential $\varphi(z)$ and the electric field $\mathbf{E}(z) = \hat{\mathbf{z}}E(z) = -z d\varphi(z)/dz$, the speed $\mathbf{v}_i(z) = \hat{\mathbf{z}}v_i(z)$ and density $n_i(z)$ of the ion flow, and the electron

TABLE I. The main plasma parameters in the numerical computation.

Definition	Notation	Value
Electron temperature	T_e	1.6; 2.0; 2.9 eV
Electron bulk density	n_0	10^9 cm $^{-3}$
Neutral density	n_n	3×10^{15} cm $^{-3}$
Neutral temperature	T_n	0.025
Ion temperature	T_i	0.025
Ion mass (argon)	m_i	$40 \times 1836 \times m_e$
Electron Debye length	λ_{De}	297.3; 332.5; 400.3 μ m
Ion Debye length	λ_{Di}	37.17 μ m
Ion plasma frequency	ω_{pi}	6.58×10^6 s $^{-1}$
Ionization frequency	ν_{ion}	0.001; 0.01; $0.1 \times \omega_{pi}$
Collision frequency	$\bar{\nu}_E$	$0.107 \times \omega_{pi}$

density $n_e(z)$, which is supposed to be Boltzmann distributed,

$$n_e(z) = n_0 \exp\left(\frac{e\varphi(z)}{T_e}\right), \quad (1)$$

where e is the electron charge, n_0 is the electron (as well as ion) number density in the plasma bulk ($z \geq z_0$), and T_e is the electron temperature in energy units (such that the Boltzmann constant is unity). Note that for simplicity we assume that the electron temperature is constant in the whole region of interest.

The sheath potential is determined by Poisson's equation which, using Eq. (1), we write as

$$\frac{d^2\varphi(z)}{dz^2} = 4\pi en_0 \left[\exp\left(\frac{e\varphi(z)}{T_e}\right) - \frac{n_i(z)}{n_0} \right]. \quad (2)$$

In this model, we neglect the total charge contributed by the dust grains (i.e., we assume the dust number density to be small).

The ion dynamics is governed by the continuity and momentum equations. The continuity equation for the ions takes into account plasma production; the main mechanism of ionization is assumed to be electron impact ionization, so that the continuity equation is

$$\frac{d}{dz} [n_i(z)v_i(z)] = \nu_{ion}n_e(z). \quad (3)$$

Here, ν_{ion} is the plasma ionization frequency, which is proportional to the neutral gas density and varies exponentially with the inverse of T_e , as well as depending on the atomic parameters of the neutral gas [36]; for argon gas it has the form

$$\nu_{ion} = 5 \times 10^{-8} n_n \exp(-15.8/T_e), \quad (4)$$

where ν_{ion} is independent of z since we assume T_e and the neutral gas density to be uniform; n_n is measured in cm $^{-3}$ and T_e in eV. Below, we assume that the neutral background density is kept constant, so that the variation in the ionization frequency is connected with the change in the electron temperature (see Table I).

TABLE II. The boundary conditions for the numerical computation.

Ionization frequency $\nu_{\text{ion}}/\omega_{pi}$	End of simulation $z=z_0$ (units of λ_{Di})	Electric potential $e\varphi/T_e$ at $z=z_0$	Electric field $-d_z(e\varphi/T_e)$ at $z=z_0$	Ion flow velocity v_i/v_{Ti} at $z=z_0$
0.001	813.05	-0.0001	-0.0001	0.25
0.01	294.56	-0.0001	-0.0001	0.25
0.1	113.32	-0.0001	-0.0001	0.25

The momentum equation for the plasma ions is written as

$$m_i v_i(z) \frac{dv_i(z)}{dz} = -e \frac{d\varphi(z)}{dz} - F_{\text{coll}}(z), \quad (5)$$

where $F_{\text{coll}}(z)$ is the momentum transfer rate between ions and neutrals, and the main mechanism for the ion-neutral collisions is considered to be charge exchange. Calculations on the basis of plasma kinetic theory, which allow for ion speeds comparable to the ion thermal speed, give the following expression for F_{coll} [28]:

$$F_{\text{coll}} = \bar{\nu}_E f(\delta) v_i. \quad (6)$$

Here $\delta = |v_i|/\sqrt{2}v_{Ti}(1+T_n/T_i)^{1/2}$, $\bar{\nu}_E$ is the average charge exchange collision frequency

$$\bar{\nu}_E = \frac{8}{3} \sqrt{\frac{2}{\pi}} q_E n_n v_{Ti} \left(1 + \frac{T_n}{T_i}\right)^{1/2}, \quad (7)$$

and q_E is the characteristic charge exchange momentum transfer cross section, which is practically constant and equals approximately $3 \times 10^{-15} \text{ cm}^2$ [37] over the range of ion energies from 0.1 to 2 eV, which is of the most interest for us here. Furthermore, n_n in Eq. (7) is the density of the neutral gas (argon), $v_{Ti} = (T_i/m_i)^{1/2}$ is the ion thermal velocity, and $T_{i(n)}$ is the ion (neutral) temperature. In our consideration, we assume n_n , T_i , and T_n to be uniform, i.e., inde-

pendent of the position z with respect to the electrode. Finally, the function $f(\delta)$ in Eq. (6) is given by [28],

$$f(\delta) = \frac{3}{8\delta^3} \left[\left(\delta^3 + \frac{\delta}{2} \right) \exp(-\delta^2) + \frac{\sqrt{\pi}}{\delta} \left(\delta^5 + \delta^3 - \frac{\delta}{4} \right) \text{erf}(\delta) \right]. \quad (8)$$

For small δ (low ion speeds), F_{coll} is proportional to the ion speed, while for large δ (high ion speeds), the approximation made in Ref. [25], F_{coll} is proportional to the square of the ion speed. The latter case applies in the sheath region in the calculations reported here, but not necessarily in the plasma bulk region.

Assuming the electrode has a potential of -7 V, typical of dust plasma experiments, Eqs. (2), (3), and (5) are numerically integrated to give the dependence of the potential, and thence of the sheath electric field, on z . Table I gives the values of the plasma parameters chosen in our numerical simulations [as well as some characteristic values which are calculated on their basis, i.e., the electron (ion) Debye lengths $\lambda_{De(i)} = (T_{e(i)}/4\pi n_0 e^2)^{1/2}$ and the ion plasma frequency $\omega_{pi} = (4\pi n_0 e^2/m_i)^{1/2}$ in the plasma bulk]. The boundary conditions are chosen as those given in Table II; note that we also have $n_e(z_0) = n_i(z_0) = n_0$.

The results for the electrostatic potential and for the electric field are given in Fig. 2, where we present three sets of figures corresponding to different ratios of the ionization fre-

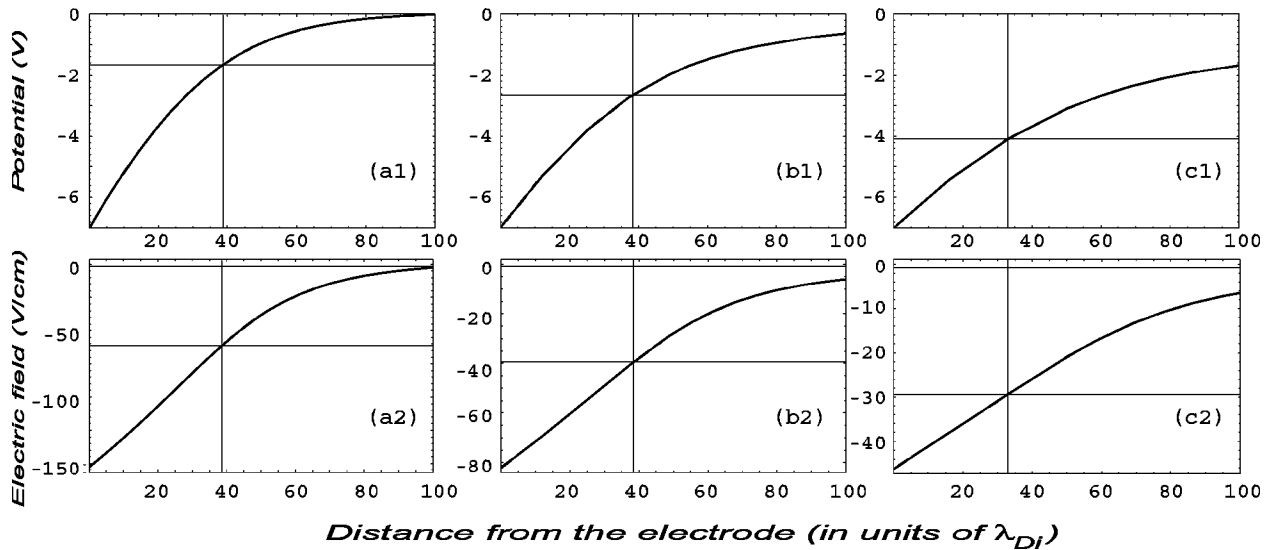


FIG. 2. The dependence of the plasma potential $\varphi(z)$ [in V, (a1)–(c1)] and the electric field $E(z)$ [in V/cm, (a2)–(c2)], on the distance $h = z/\lambda_{Di}$ (in units of the ion Debye length for all figures) from the electrode. (a1),(a2) correspond to $\nu_{\text{ion}}/\omega_{pi} = 0.1$, (b1),(b2) correspond to $\nu_{\text{ion}}/\omega_{pi} = 0.01$, and (c1),(c2) correspond to $\nu_{\text{ion}}/\omega_{pi} = 0.001$. The plasma parameters are presented in Table I. The vertical and horizontal lines in the figures indicate the points where the ion flow velocity equals the ion sound velocity v_s ; the corresponding values of electric field and potential relevant for Fig. 2 are given in Table III.

TABLE III. The characteristic numbers for Fig. 2.

Ionization frequency $\nu_{\text{ion}}/\omega_{pi}$	Position where ion flow speed = v_s (units of λ_{Di})	Electric field at the electrode (units of V/cm)	Electric field at $v_i = v_s$ (units of V/cm)	Potential at $v_i = v_s$ (units of V)
0.1	38.56	-152.9	-61.3	-1.66
0.01	38.38	-82.1	-39.5	-2.64
0.001	32.93	-46.2	-29.4	-4.10

quency to the ion plasma frequency $\nu_{\text{ion}}/\omega_{pi}$, viz., 0.1, 0.01, and 0.001, respectively. The first case corresponds to highest T_e and input power. The vertical and horizontal lines in the figures indicate the points where the ion flow velocity equals the ion sound velocity v_s ; the corresponding values of electric field and potential relevant for Fig. 2 are given in Table III.

The dependences of the velocity of the ion flow $v_i(z)$ and the ion flux $n_i(z)v_i(z)$ on the distance from the electrode, found from Eq. (5), for the potential and field distributions of Fig. 2, are presented in Fig. 3. Again the vertical and horizontal lines in the figures indicate the points where the ion flow velocity equals the ion sound velocity v_s ; the corresponding ion flux, as well as other characteristic parameters relevant for Fig. 3, are given in Table IV.

We see that for the region where the ion velocity Mach number (relative to the ion sound velocity v_s) exceeds unity (this corresponds, for the chosen plasma parameters, to $v_i > v_s \sim 10v_{Ti}$), the ion flux is almost constant. Moreover, comparing with Fig. 2, we see that this region corresponds to an almost linear electric field dependence on the distance from the electrode, resembling the collisionless sheath model (which we discussed in [33]) where the region of almost linear dependence of the electric field is, however, limited to somewhat higher velocities of the flow.

III. CHARGE AND EQUILIBRIUM OF A DUST GRAIN

The charge Q of the dust particles (which is dependent on the plasma parameters, in particular, on the local electric sheath potential and the velocity of the ion flow) is found from the condition of zero total plasma current onto the grain surface:

$$I(Q) = I_e(Q) + I_i(Q) = 0. \quad (9)$$

Note that, since we are interested in collective processes on the time scale of the characteristic frequencies (of order a few times 10 s^{-1}), which are much lower than the charging frequency [38] (which can be of order 10^5 s^{-1}), we assume that (re)charging of dust grains is practically instantaneous, and we therefore neglect the charging dynamics. We note, however, that the latter can be important when considering possible instabilities of the grain levitation associated with the charging dynamics [39].

The electron and ion currents onto the dust grain are defined by

$$I_\alpha(Q) = \sum_\alpha \int e_\alpha f_\alpha \sigma_\alpha(v, Q) v d\mathbf{v}. \quad (10)$$

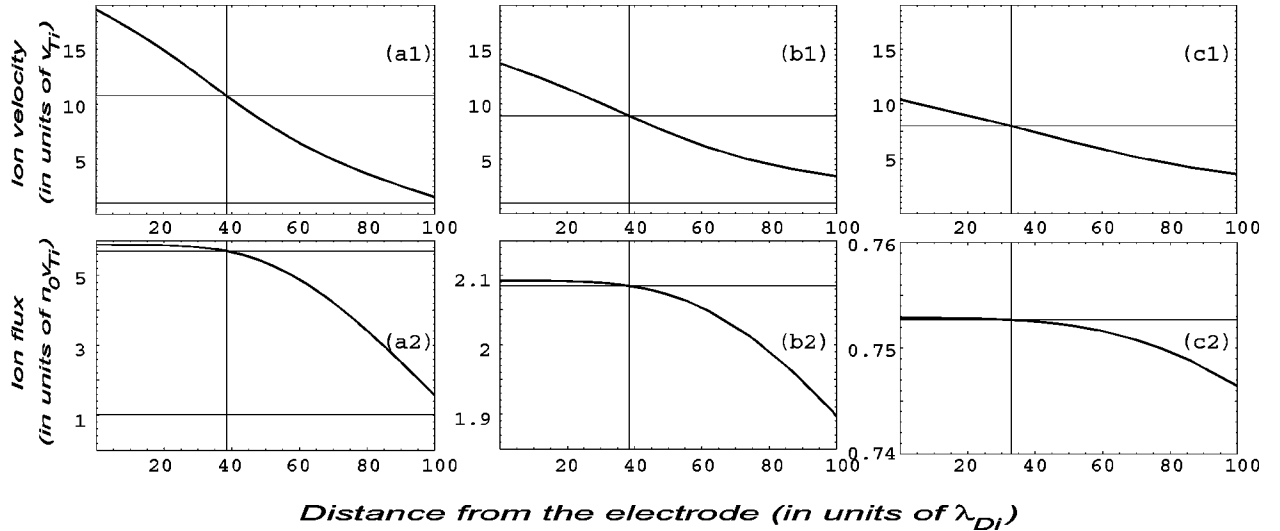


FIG. 3. The dependence of the velocity $v_i(z)$ [in units of v_{Ti} , (a1)–(c1)] of the ion flow and the ion flux $n_i(z)v_i(z)$ [in units of n_0v_{Ti} , (a2)–(c2)] on the distance $h = z/\lambda_{Di}$ (in units of the ion Debye length for all figures) from the electrode. (a1),(a2) correspond to $\nu_{\text{ion}}/\omega_{pi} = 0.1$, (b1),(b2) correspond to $\nu_{\text{ion}}/\omega_{pi} = 0.01$, and (c1),(c2) correspond to $\nu_{\text{ion}}/\omega_{pi} = 0.001$. The vertical and horizontal lines in the figures indicate the points where the ion flow velocity equals the ion sound velocity v_s ; the corresponding ion flux, as well as other characteristic parameters relevant for Fig. 3, are given in Table 4.

TABLE IV. The characteristic numbers for Fig. 3.

Ionization frequency $\nu_{\text{ion}}/\omega_{pi}$	Ion velocity at the electrode (units of v_{Ti})	Ion flux at the electrode (units of $n_0 v_{Ti}$)	Ion flux at $v_i = v_s$ (units of $n_0 v_{Ti}$)	Position where ion flow speed = v_{Ti} (units of λ_{Di})
0.1	18.60	5.8774	5.6946	105.46
0.01	13.73	2.0923	2.0846	224.01
0.001	10.38	0.7529	0.7527	361.00

Here, the subscript $\alpha = e, i$ stands for electrons or ions, e_α and f_α are the charge and distribution function of the plasma particles, with $e_e = -e_i = -e$, $v = |\mathbf{v}|$ is the absolute value of the particle speed \mathbf{v} , and σ_α is the charging cross section, which in the orbit-limited-motion (OLM) approximation is given by [40]

$$\sigma_\alpha = \begin{cases} \pi a^2 \left(1 - \frac{2e_\alpha Q}{am_\alpha v^2} \right) & \text{if } \frac{2e_\alpha Q}{am_\alpha v^2} < 1 \\ 0 & \text{if } \frac{2e_\alpha Q}{am_\alpha v^2} \geq 1, \end{cases} \quad (11)$$

where a is the radius of the dust particle and m_α is the electron or ion mass. The last inequality in Eq. (11) gives a restriction on the electron charging velocities for negatively charged dust particles or for the plasma (positive) ions for positively charged dust grains.

Since the electrons are assumed to be Boltzmann distributed [Eq. (1)], the electron current (for a negative charge on the dust grain) is given by

$$I_e(Q) = -\sqrt{8\pi} e a^2 n_0 \sqrt{\frac{T_e}{m_e}} \exp\left(\frac{eQ(z)}{aT_e} + \frac{e\varphi(z)}{T_e}\right), \quad (12)$$

where $\varphi(z)$ is the external plasma potential at the position of the dust grain. Note that we neglect possible changes of the electron temperature in the plasma sheath.

In contrast to the electron distribution, we consider shifted Maxwellian ions with the distribution function $f_i \propto \exp\{-[v_z - v_i(z)]^2/v_{Ti}^2\}$. The intergrain distance is assumed to be not less than the (electron) Debye length, so that the ion trajectory is affected by only a single grain. The ion current onto the dust grain in this case can be approximated by

$$I_i = \pi a^2 e n_i(z) \bar{v}_i(z) \left(1 - \frac{2eQ(z)}{am_i \bar{v}_i^2(z)} \right), \quad (13)$$

where $\bar{v}_i(z) = \sqrt{v_i^2(z) + 8v_{Ti}^2/\pi}$ [41]. Thus the charge of a (negatively charged) dust particle is determined by Eq. (9), i.e., by the equation

$$\begin{aligned} & \sqrt{\pi/8} n_i(z) \bar{v}_i(z) \left(1 - \frac{2eQ(z)}{am_i \bar{v}_i^2(z)} \right) \\ &= n_0 v_{Te} \exp\left(\frac{eQ(z)}{aT_e} + \frac{e\varphi(z)}{T_e}\right), \end{aligned} \quad (14)$$

where $v_{Te}^2 = T_e/m_e$ is the squared electron thermal speed. We note that from Eq. (14) the charge can become zero for a strong enough sheath potential, such that the ion current dominates. This means that the dust particle cannot levitate

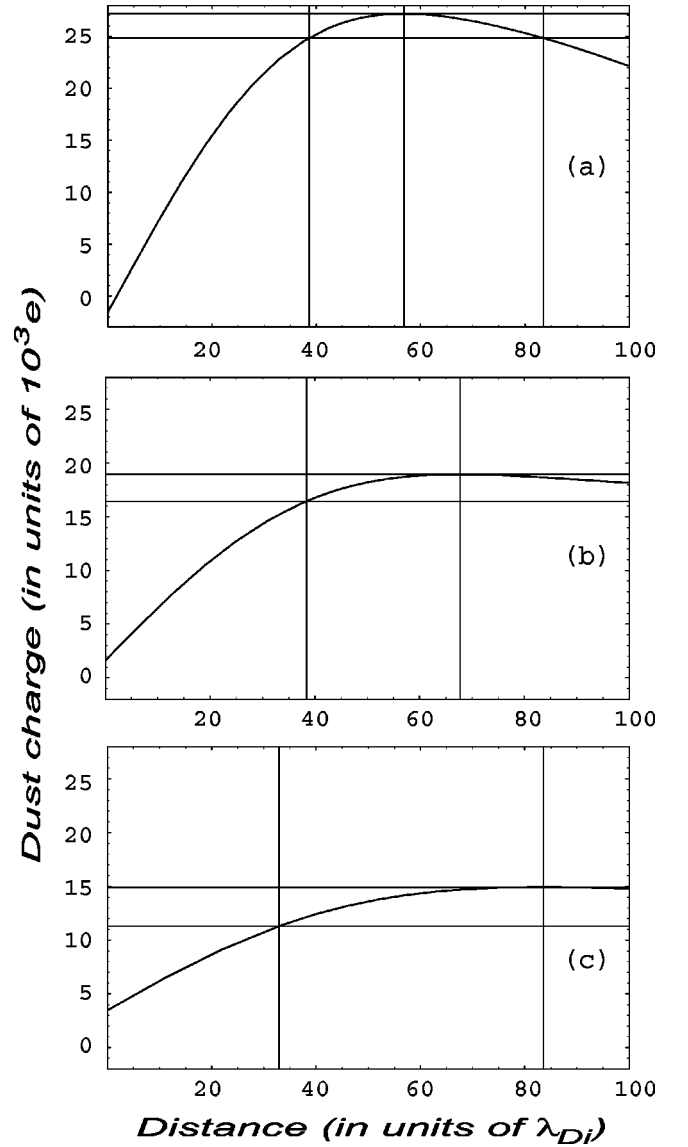


FIG. 4. The dependence of the charge $q = -(Q/e) \times 10^{-3}$ of the dust grain, of radius $a = 4 \mu\text{m}$, on the grain position $h = z/\lambda_{Di}$. Here we have (a) $\nu_{\text{ion}}/\omega_{pi} = 0.1$, (b) $\nu_{\text{ion}}/\omega_{pi} = 0.01$, and (c) $\nu_{\text{ion}}/\omega_{pi} = 0.001$. The characteristic values of the charge at various positions, as well as the position for the maximum possible charge, are summarized in Table V. The vertical and horizontal lines indicate the position of maximum charge, and the charge where $v_i = v_s$.

TABLE V. The characteristic numbers for the dust charge calculation (Fig. 4).

Ionization frequency $\nu_{\text{ion}}/\omega_{pi}$	Charge at the electrode q_0 (units of $10^3 e$)	Maximum possible charge q_{max} (units of $10^3 e$)	Position of q_{max} z_{qm} (units of λ_{Di})	Charge at the position $v_i=v_s$ q_{vs} (units of $10^3 e$)	Charge at the position $v_i=v_{Ti}$ q_{vT} (units of $10^3 e$)
0.1	(-)	27.19	56.77	24.84	20.11
0.01	1.64	18.96	67.77	16.46	14.72
0.001	3.46	14.91	83.60	11.31	

and must fall onto the electrode (see the discussion in Ref. [33]). Numerical solutions of Eq. (14) for the charge of a dust particle, as a function of the particle position z , are presented in Fig. 4, for the example of a dust grain of radius $a=4 \mu\text{m}$. Here the profiles of $\phi(z)$, $v_i(z)$, and $n_i(z)$ found in Sec. II have been used. The characteristic values of the charge at various positions, as well as the position for the maximum possible charge, are summarized in Table V. The vertical and horizontal lines indicate the position of maximum charge, and the charge where $v_i=v_s$ [Figs. 4(a), 4(b), and 4(c)]. An extra line in Fig. 4(a) indicates that in general there are two positions for a charge of less than the maximum charge.

It is apparent from Fig. 3 that the higher is the input power (i.e., the higher T_e and ν_{ion}), the stronger are the ion fluxes, and, correspondingly, the lower is the size of the negative charge on a grain placed very close to the electrode. Note that the dust charge can even become positive; in the case $\nu_{\text{ion}}=0.1\omega_{pi}$, the dust charge becomes positive near the electrode, with the result that no (equilibrium) levitation is possible. The maximum possible size of the charge is larger for a higher level of ionization rate; the position of the maximum charge size becomes closer to the electrode as the ionization rate increases. We note also that the negative gradient of the equilibrium charge [i.e., $dQ(z)/dz < 0$] can lead to an instability of dust particles with respect to their vertical oscillations due to delayed charging [39].

For a particle levitating in the sheath field, the force acting on the grain includes the sheath electrostatic force, the ion drag force, and gravity:

$$F(z) = Q(z)E(z) - F_{i,\text{dr}}(z) - m_d g, \quad (15)$$

where the ion drag force $F_{i,\text{dr}}(z) = F_{i,\text{dr}}^{\text{col}}(z) + F_{i,\text{dr}}^{\text{orb}}(z)$ includes two components [41,42], the collection force $F_{i,\text{dr}}^{\text{col}}(z)$ and the orbit force $F_{i,\text{dr}}^{\text{orb}}(z)$. The collection force is associated with the dust charging process, and in the OLM approximation can be written as

$$F_{i,\text{dr}}^{\text{col}}(z) = \pi a^2 m_i \bar{v}_i(z) v_i(z) \left(1 - \frac{2eQ(z)}{am_i \bar{v}_i^2(z)} \right). \quad (16)$$

The orbit force, which corresponds to the momentum transfer during the Coulomb collision, is given by

$$F_{i,\text{dr}}^{\text{orb}}(z) = 4\pi e^2 Q^2(z) \frac{n_i(z)v_i(z)}{m_i \bar{v}_i^3(z)} \Lambda, \quad (17)$$

where $\Lambda \approx \ln(\lambda_D/a)$ is the Coulomb logarithm, and λ_D is the plasma Debye length.

Note that the force (15) includes the z dependence of the grain charge Q , since we assume instantaneous transfer of charge onto and off the dust grain at any grain position in the sheath, such that Eq. (14) is always satisfied. The balance of

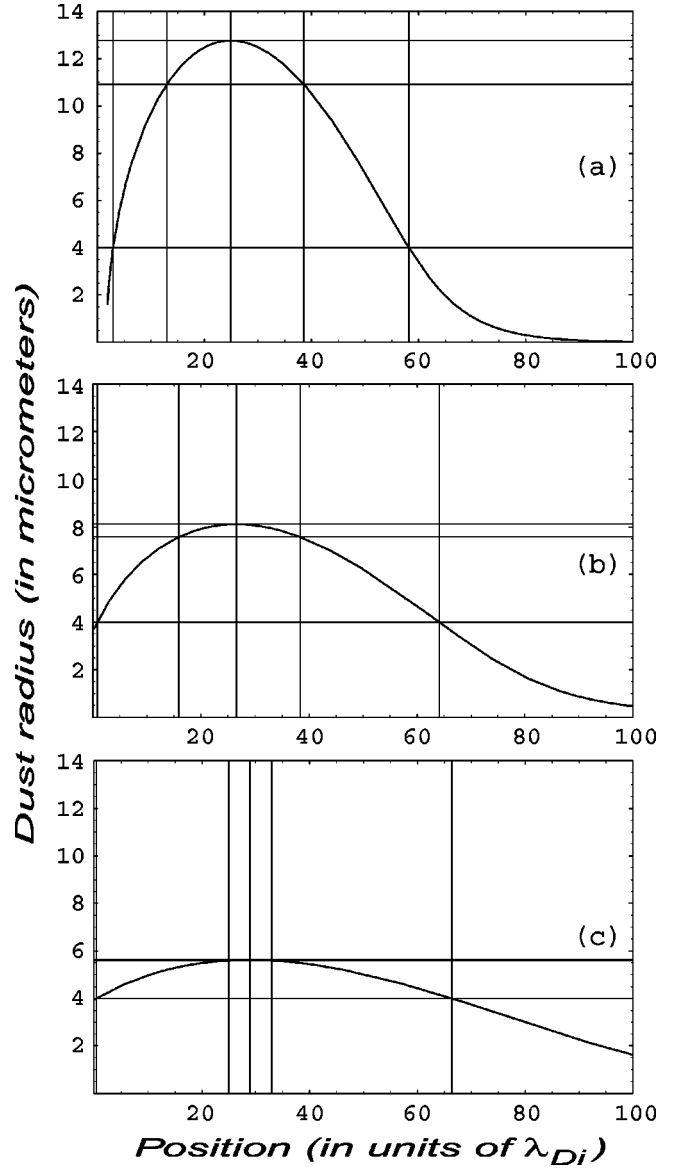


FIG. 5. The dependence of the size of the dust grain (in μm), levitating in the sheath electric field, on its position $h = z/\lambda_{Di}$. Here we have (a) $\nu_{\text{ion}}/\omega_{pi}=0.1$, (b) $\nu_{\text{ion}}/\omega_{pi}=0.01$, and (c) $\nu_{\text{ion}}/\omega_{pi}=0.001$. The lines correspond to various sizes of dust grains: as an example, $a=4 \mu\text{m}$, as well as the maximum possible sizes, and the sizes corresponding to a grain levitating at the position where the Mach number of the ion flow is unity (i.e., at $v_i=v_s$), as summarized in Table VI.

TABLE VI. The characteristic numbers for the dust grain radius and the position of dust levitation (Fig. 5).

Ionization frequency $\nu_{\text{ion}}/\omega_{pi}$	Maximum grain radius $a_{\text{max}} (\mu\text{m})$	Position of the grain a_{max} z_{am} (units of λ_{Di})	Radius of the grain at $v_i=v_s$ $a_{vs}(\mu\text{m})$	Positions of a grain of radius $4\mu\text{m}$ (units of λ_{Di})	Unstable positions of the grain a_{vs} (units of λ_{Di})
0.1	12.77	24.93	10.92	58.14(2.93)	12.97
0.01	8.11	26.55	7.57	64.11(0.78)	15.89
0.001	5.62	28.87	5.60	66.41(0.43)	24.93

forces in the vertical direction is

$$Q(z)E(z) = m_{dg} + F_{i,\text{dr}}(z). \quad (18)$$

Solution of this equation together with the charging equation (14) gives the dependence of the charge of the grain, levitating in the sheath electric field, as a function of its size. For the levitating dust particle, there is therefore a one-to-one correspondence of its size to its equilibrium position of levitation in the sheath, as shown in Fig. 5. Here, we have also plotted the lines corresponding to various sizes of dust grains: as an example, $a=4\mu\text{m}$, as well as the maximum possible sizes, and the sizes corresponding to a grain levitating at the position where the Mach number of the ion flow is unity (i.e., at $v_i=v_s$), as summarized in Table VI. Note that there are no equilibrium solutions for $a>a_{\text{max}}$, the latter being a function of the ionization rate (see Table VI). The absence of an equilibrium means that the particles with such sizes will fall down onto the electrode.

From Fig. 5 and Table VI, we see that the greater is the ionization rate, the closer is the equilibrium position of a levitating dust grain to the electrode. This fact agrees with experimental observations (e.g., [9,11]) showing that the size of a dust void is directly proportional to the ionization rate. The void corresponds to a dust-free region where the electron impact ionization rate is relatively high, producing an outward electric field and ion flow, thus dragging the dust particles outward. In the case discussed in this paper, a higher ionization rate again gives a stronger ion flow, dragging the dust grain closer to the electrode. Note that if there are two positions for a grain of a given radius (e.g., $4\mu\text{m}$ in Fig. 5), the one with a negative derivative $da(z)/dz$ is stable, while the one with a positive derivative is unstable (see also the next section). We also note that the maximum possible radius for grain levitation increases with increase of the ionization rate, and its position also shifts closer to the electrode. Finally, we see that the smaller is the ionization rate, the smaller is the maximum possible size a_{max} of a grain capable of levitating, and therefore the greater is the proportion of dust (if there is a dispersion of grain sizes) levitating in the region of subsonic ion flow velocities, i.e., in the presheath region.

IV. DISCUSSION AND CONCLUSION

It is instructive to find the total potential energy, relative to the electrode position, of a single dust particle of given size at the position z in the sheath electric field:

$$U_{\text{tot}}(z) = - \int_0^z dz' [Q(z')E(z') - F_{i,\text{dr}}(z') - m_{dg}]. \quad (19)$$

Note that the total energy in this case contains not only the electrostatic energy $Q(z)\varphi(z)$, but also terms associated with $dQ/d\varphi$ which represent, because of the openness of the system, the work of external forces that change the dust charge. The dependence of the total potential energy on the distance from the electrode is shown in Fig. 6.

We see that the potential has a maximum and a minimum, corresponding to the two equilibrium positions found in Sec. III. The minimum (the stable equilibrium) disappears if $a > a_{\text{max}}$ [the curve (1) in Fig. 6]. Other effects that have been neglected here, such as an electron temperature increasing toward the electrode, may serve to increase the negative charge on a grain, and so preserve an equilibrium. The critical (maximum possible for levitation) radius appears also in Fig. 5; for decreasing ionization rate, a_{max} also decreases (see Table VI). For $a > a_{\text{max}}$, the minimum of the potential energy curve disappears, thus indicating that there is no equilibrium position for such grain sizes.

Thus for a collisional plasma with an ionization source, for a grain size a less than the critical radius a_{max} , there is a stable equilibrium position close to (or in) the presheath; for sufficiently high input powers (within a certain range of grain sizes, see Fig. 5), there can also be an unstable equilibrium position deeper inside the sheath. For a greater than the critical radius a_{max} , there is no equilibrium position. Note that possible vertical oscillations about the stable equilibrium may develop high amplitudes, thus leading to a fall of the oscillating grain onto the electrode when the potential barrier is overcome (see Fig. 6).

Here, we would like to discuss how the change of the ionization power can affect dust size distributions in an experiment. Suppose that we start with a low ionization power and then *increase* it in the process of the experiment. Since the maximum possible size of particles capable of levitating in this case is only *increasing*, no change of dust size distribution occurs, with dust levitating closer to the electrode as the input power increases. However, if in the next experiment we *decrease* the ionization power, the possible size of particles capable of levitating is also *decreasing*, with the heaviest grains (whose size and, correspondingly, mass do not satisfy the condition for levitation) falling down to the electrode. Thus the dust size (and mass) distribution can be changed in this way, leaving only smaller particles levitating. Note also that another experimental possibility to force bigger particles (whose sizes are close to the critical one) to fall down to the electrode is to apply a low-frequency-modulated

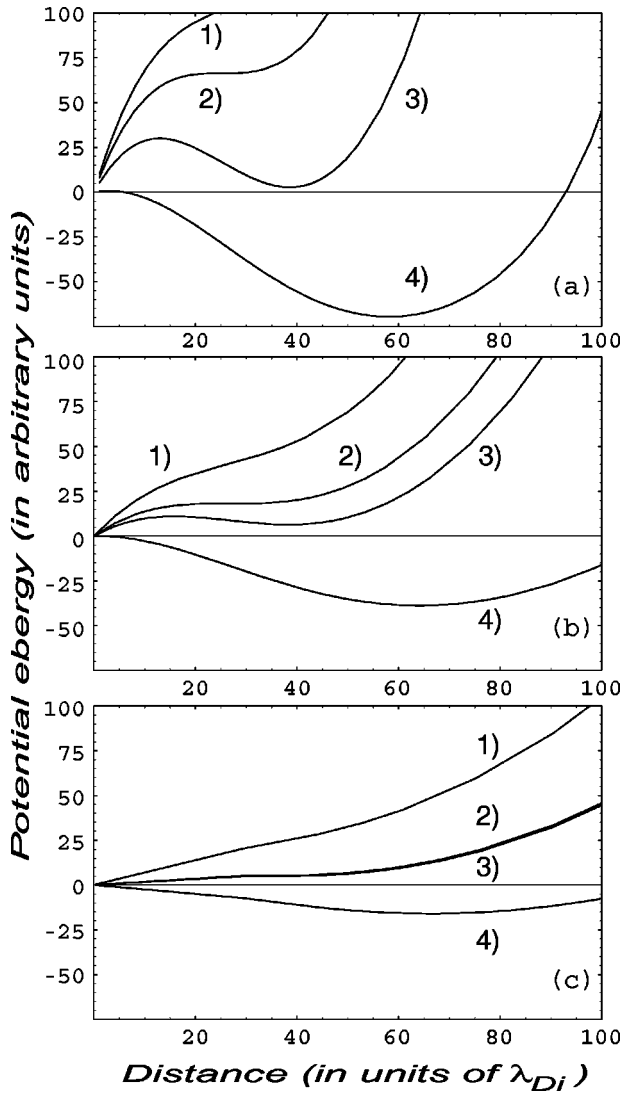


FIG. 6. The total interaction energy U_{tot} as a function of the distance $h = z/\lambda_{Di}$ from the electrode for the different sizes of a dust particle and the different ionization rates: (a) $\nu_{\text{ion}}/\omega_{pi} = 0.1$, (b) $\nu_{\text{ion}}/\omega_{pi} = 0.01$, and (c) $\nu_{\text{ion}}/\omega_{pi} = 0.001$. The curves correspond to (1) $a = a_{\text{max}} + 1 \mu\text{m}$; (2) $a = a_{\text{max}}$; (3) $a = a_{vs}$; and (4) $a = 4 \mu\text{m}$. See also Fig. 5 and Table VI.

voltage (with the frequency close to the resonant frequency of vertical vibrations of the dust grains around the equilibrium position [33–35]) to the lower electrode, thus forcing particles to oscillate. When their amplitude (and therefore the energy of oscillations) becomes large enough to overcome the potential barrier, cf. Fig. 6, they fall down and therefore are removed from the sheath region.

We assumed that the dust density is small enough not to influence significantly the plasma parameters (such as electric field, etc.). The performed study has also demonstrated some qualitative features of dust trapping and equilibrium for those experiments (e.g., on void formation [9,11]) where the dust density is higher. We can therefore qualitatively conclude that the effects of single particle trapping and equilibrium are important also for the levitation of dust distributions. For dust clouds, there are several physical effects important for particle trapping and equilibrium, among which are the change of the plasma electric field, density, etc., dis-

tributions due to the charged dust cloud [10,12], and the change (decrease) of the charge of a dust particle due to the presence of neighboring grains in the cloud [43,44]. The quantitative answer to the question of the differences between a dense dust cloud and isolated dust particle trapping can be given only after the corresponding theory for the dust distributions is developed.

Another issue is the influence of the ion flow effects on the stability and equilibrium of dust grains. For an adequate description of the effects of ion wake formation [14–16], a treatment taking into account plasma ion kinetics is necessary. The hydrodynamic model studied here is not able to take those effects into account. However, it is physically clear that for a monolayer dust distribution (in the plane of the electrode) the wake effects are not important. On the other hand for a highly collisional plasma the wake effects are not strong if the ion-neutral mean free path is of the order of the plasma Debye length, when the ion focusing is destabilized by frequent ion-neutral collisions. Similarly, for sufficiently dense dust distributions the plasma ion kinetics can be effective only for a layer near the dust-cloud-void boundary, of the order of the ion-dust (or the ion-neutral, whichever is smaller) mean free path. However, a comprehensive theory of the wake formation in collisional plasmas, for those situations when estimations may predict considerable wake effects, does not exist at the moment.

In our calculations, we assumed the major influence on the ionization source to be the plasma electron temperature, and kept the neutral density constant for all runs. One of the reasons for such a choice is that according to Eq. (4) the effective ionization frequency varies exponentially with the inverse of T_e and is only directly proportional to the neutral gas density. Thus for relatively small changes of the electron temperature we have two orders of magnitude change in the effective ionization frequency; cf. Table I. Note that the associated change of the dust particle charges is not so sensitive to the electron temperature (see Fig. 4). Varying the electron temperature but keeping the neutral number density constant, for a collisional weakly ionized plasma, effectively means changing the input power while keeping the pressure constant, since the neutral temperature does not differ much from the room temperature in this case. On the other hand, it is also possible to check the ionization effects of varying the neutral density [which does not directly appear in the charging equation (9) and is therefore expected to less directly affect the grain charges], which corresponds to varying the ionization input power together with the pressure of the discharge.

A complete model, which is beyond the scope of this paper, would include the whole calculation of the discharge parameters as functions of the input power, taking into account changes of both the neutral density and the plasma electron temperature. In the model considered here, we assumed that the temperatures of plasma electrons and ions are constant in the simulation region. Note that more complicated models of plasma discharges [45–47] take into account the dependence of the temperatures on the distance from the electrode. For a dusty plasma, this is a subject for future studies: e.g., our model can be further complicated by the inclusion of extra equations for the balance of the temperatures of plasma electrons and ions. Note that in this case the

physics of the electrostatic dust-plasma interactions in the sheath region can include extra forces of a thermophoretic type due to the plasma particle temperature gradients [48].

To conclude, we have demonstrated that the charge, position, and trapping of dust grains levitating in a collisional plasma with an ionization source, in the electric field of a horizontal negatively biased electrode, strongly depend on the parameters of the plasma as well as on the input power.

The dependence of the grain charge on its position is crucial for the stability, equilibrium, and trapping of the dust particles.

ACKNOWLEDGMENT

This work was supported by the Australian Research Council.

-
- [1] J.H. Chu and Lin I, Phys. Rev. Lett. **72**, 4009 (1994).
 [2] H. Thomas, G.E. Morfill, V. Demmel, J. Goree, B. Feuerbacher, and D. Möhlmann, Phys. Rev. Lett. **73**, 652 (1994).
 [3] Y. Hayashi and K. Tachibana, Jpn. J. Appl. Phys., Part 2 **33**, L804 (1994).
 [4] A. Melzer, T. Trottenberg, and A. Piel, Phys. Lett. A **191**, 301 (1994).
 [5] H.M. Thomas and G.E. Morfill, Nature (London) **379**, 806 (1996).
 [6] V.N. Tsytovich, Usp. Fiz. Nauk **167**, 57 (1997) [Phys. Usp. **40**, 53 (1997)].
 [7] S. Nunomura, N. Ohno, and S. Takamura, Phys. Plasmas **5**, 3517 (1998).
 [8] G. Praburam and J. Goree, Phys. Plasmas **3**, 1212 (1996).
 [9] D. Samsonov and J. Goree, Phys. Rev. E **59**, 1047 (1999).
 [10] J. Goree, G.E. Morfill, V.N. Tsytovich, and S.V. Vladimirov, Phys. Rev. E **59**, 7055 (1999).
 [11] G.E. Morfill, H.M. Thomas, U. Konopka, H. Rothermel, M. Zuzic, A. Ivlev, and J. Goree, Phys. Rev. Lett. **83**, 1598 (1999).
 [12] V.N. Tsytovich, S.V. Vladimirov, and S. Benkadda, Phys. Plasmas **6**, 2972 (1999).
 [13] N. Prior and L. Mitchell, unpublished.
 [14] S.V. Vladimirov and M. Nambu, Phys. Rev. E **52**, 2172 (1995).
 [15] S.V. Vladimirov and O. Ishihara, Phys. Plasmas **3**, 444 (1996).
 [16] O. Ishihara and S.V. Vladimirov, Phys. Plasmas **4**, 69 (1997); Phys. Rev. E **57**, 3392 (1998).
 [17] O. Ishihara, Phys. Rev. E **58**, 3733 (1998).
 [18] S. Benkadda, V.N. Tsytovich, and S.V. Vladimirov, Phys. Rev. E **60**, 4708 (1999).
 [19] S.V. Vladimirov and O. Ishihara, Phys. Scr. **60**, 370 (1999).
 [20] H. Totsuji, T. Kishimoto, and Ch. Totsuji, Phys. Rev. Lett. **78**, 3113 (1997).
 [21] E.C. Whipple, Rep. Prog. Phys. **44**, 1197 (1981).
 [22] F.F. Chen, *Introduction to Plasma Physics and Controlled Fusion* (Plenum, New York, 1984), Vol. 1, pp. 290–295.
 [23] M.A. Lieberman, IEEE Trans. Plasma Sci. **16**, 638 (1988).
 [24] V.A. Godyak and N. Sternberg, IEEE Trans. Plasma Sci. **18**, 159 (1990).
 [25] T. Nitter, Plasma Sources Sci. Technol. **5**, 93 (1996).
 [26] M.A. Lieberman, IEEE Trans. Plasma Sci. **17**, 338 (1989).
 [27] T.E. Sheridan and J. Goree, Phys. Fluids B **3**, 2796 (1991).
 [28] J. Horwitz and P.M. Banks, Planet. Space Sci. **21**, 1975 (1973).
 [29] T.J. Sommerer, M.S. Barnes, J.H. Keller, M.J. McCaughey, and M.J. Kushner, Appl. Phys. Lett. **59**, 638 (1991).
 [30] J.P. Boeuf, P. Belenguer, and T. Hbid, Plasma Sources Sci. Technol. **3**, 407 (1994).
 [31] D.B. Graves, J.E. Daugherty, M.D. Kilgore, and R.K. Porteous, Plasma Sources Sci. Technol. **3**, 433 (1994).
 [32] J.X. Ma, J. Liu, and M.Y. Yu, Phys. Rev. E **55**, 4627 (1997).
 [33] S.V. Vladimirov, N.F. Cramer, and P.V. Shevchenko, Phys. Rev. E **60**, 7369 (1999).
 [34] S.V. Vladimirov, P.V. Shevchenko, and N.F. Cramer, Phys. Rev. E **56**, R74 (1997).
 [35] S.V. Vladimirov, P.V. Shevchenko, and N.F. Cramer, Phys. Plasmas **5**, 4 (1998); S.V. Vladimirov and N.F. Cramer, Phys. Scr. **58**, 80 (1998).
 [36] M.A. Lieberman and A.J. Lichtenberg, *Principles of Plasma Discharges and Materials Processing* (Wiley, New York, 1994), pp. 454–460.
 [37] P.M. Banks and T.E. Holzer, Planet. Space Sci. **16**, 1019 (1968).
 [38] S.V. Vladimirov, Phys. Plasmas **1**, 2762 (1994).
 [39] S. Nunomura, T. Misawa, N. Ohno, and S. Takamura, Phys. Rev. Lett. **83**, 1970 (1999).
 [40] L. Spitzer, *Physical Processes in the Interstellar Medium* (Wiley, New York, 1978).
 [41] M.S. Barnes, J.H. Keller, J.C. Forster, J.A. O'Neill, and D.K. Coultas, Phys. Rev. Lett. **68**, 313 (1992).
 [42] S.V. Vladimirov and V.N. Tsytovich, Phys. Rev. E **58**, 2415 (1998).
 [43] E.C. Whipple, T.G. Northrop, and D.A. Mendis, J. Geophys. Res. A **90**, 7405 (1985).
 [44] O. Havnes, C.K. Goertz, G.E. Morfill, E. Grün, and W. Ip, J. Geophys. Res. A **92**, 2281 (1987).
 [45] M. Surendra and D.B. Graves, IEEE Trans. Plasma Sci. **19**, 144 (1991).
 [46] M. Surendra, Plasma Sources Sci. Technol. **4**, 56 (1995).
 [47] J.D. Bukowski, D.B. Graves, and P. Vitello, J. Appl. Phys. **80**, 2614 (1996).
 [48] V.S. Tsypin, S.V. Vladimirov, M. Tendler, A.S. de Assis, and C.A. de Azevedo, Phys. Lett. A **239**, 94 (1998).